Water Research, Volume 53, 15 April 2014, Pages 168–179

THE IMPACTS OF REPLACING AIR BUBBLES WITH MICROSPHERES FOR THE CLARIFICATION OF ALGAE FROM LOW CELL-DENSITY CULTURE

FRANCESCO OMETTO[i], CARLO POZZA[ii], RACHEL WHITTON[i], BEATRICE SMYTH[iii], ANDREA GONZALEZ TORRES[iv], RITA K HENDERSON[iv], PETER JARVIS[i], BRUCE JEFFERSON[i] and RAFFAELLA VILLA[i,*]

[i] Cranfield University, Bedfordshire, UK;

[ii] University of Duisburg-Essen, Essen, DE;

[iii] Queen's University, Belfast, UK;

[iv] The University of New South Wales, Sydney, AU;

[*] Corresponding author: r.villa@cranfield.ac.uk

Water Res. 2014 Apr 15;53:168-79. doi: 10.1016/j.watres.2014.01.012.

Abstract

Dissolved Air Flotation (DAF) is a well-known coagulation-flotation system applied at large scale for microalgae harvesting. Compared to conventional harvesting technologies DAF allows high cell recovery at lower energy demand. By replacing microbubbles with microspheres, the innovative Ballasted Dissolved Air Flotation (BDAF) technique has been reported to achieve the same algae cell removal efficiency, while saving up to 80% of the energy required for the conventional DAF unit. Using three different algae cultures (*Scenedesmus obliquus*, *Chlorella vulgaris* and *Arthrospira maxima*), the present work investigated the practical, economic and environmental advantages of the BDAF system compared to the DAF system. 99 % cells separation was achieved with both systems, nevertheless, the BDAF technology allowed up to 95 % coagulant reduction depending on the

algae species and the pH conditions adopted. In terms of floc structure and strength, the inclusion of microspheres in the algae floc generated a looser aggregate, showing a more compact structure within single cell alga, than large and filamentous cells. Overall, BDAF appeared to be a more reliable and sustainable harvesting system than DAF, as it allowed equal cells recovery reducing energy inputs, coagulant demand and carbon emissions.

Key words: microalgae harvesting; dissolved air flotation; ballasted flotation; floc structure; carbon footprint;

1 Introduction

Algae harvesting optimisation is a fundamental need for the feasibility of third generation biofuels (biodiesel, bioethanol, biohydrogen and biogas from microalgae) (Lee, 2011). This is most apparent in the cases where algae are grown in wastewater to provide a dual benefit of nutrient removal and biofuel generation. A reduction of the energy and costs associated with this process has the potential to make algae-biofuels more economically competitive in the market (Molina Grima *et al.,* 2003). Furthermore, as carbon emissions are becoming an important factor in decision making in the water/energy sector (OFWAT, 2010), more sustainable technologies are required to provide environmental benefits often measured in terms of reduced carbon footprint.

Centrifuges, membrane filtration and flocculation-flotation units are the common harvesting systems applied in large scale culture (Christenson and Sims, 2011). While the energy demand for centrifuges or pressure and vacuum filters ranges between 1 and 8 kWh m^{-3} of treated water, flocculation-flotation configurations require lower energy inputs (0.1 and 0.5 kWh m^{-3}) which has seen progressing increase in research related to flocculation-flotation systems in recent years (Rawat *et al.,* 2013; Molina Grima *et al.,* 2003). In the Dissolved Air Flotation (DAF) system, micro-bubbles attached to the pre-flocculated algal biomass, float the algae floc to the surface allowing high cell recovery (Rawat *et al.,* 2013; Edzwald, 1993) (Figure 1A). The efficiency of this process, as in all flocculation-flotation treatments, relies on floc formation which is affected by particle morphology, suspension characteristics and coagulant properties (Pieterse and Cloot, 1997). In particular, the extracellular algogenic organic matter (AOM) of the suspension plays a key role in coagulant demand and floc structure and strength (Li *et al.,* 2012; Henderson *et al.,* 2010). AOM is composed predominantly of carbohydrates (hydrophilic) and proteins (hydrophobic) and has a negative charge (≤ -15 mV) depending on the algal strain and its growth phase (Henderson *et al.,*

2008a). Optimal coagulant doses allow floc formation to be able to resist the shear rate generated during saturated flow injection (450-600 kPa) and have been observed to occur at zeta potential values close to +/- 0 mV where the coagulant is responsible for particle charge neutralisation (Henderson *et al.*, 2008a).

A modified DAF system, Ballasted Dissolved Air Flotation (BDAF), has been reported to achieve the same removal efficiency while saving from 60 to 80% of the energy demand, and related CO_2 emissions, compared to conventional flotation units (Jarvis *et al.*, 2009). Unlike traditional ballasting techniques where high density granular additives (e.g. microsand) are used to improve sedimentation efficiency (Desjardins *et al.*, 2002), BDAF uses low-density microspheres to support flotation (Figure 1B). Microspheres are added into the system during the rapid mix stage in the same way as conventional ballasting agents, and then incorporated into the floc matrix to drive the flotation process, replacing the use of microbubbles (WO/2006/008474 and US Patent 6890431). Once the algae-bead floc has been harvested, the microspheres can be separated from the algal biomass and recycled into the system. The effect of low density glass microsphere addition on the pre-flocculation process was first investigated by Jarvis *et al.* (2009), who identified an optimal glass beads concentration close to 300 mg l^{-1} for harvesting an algae cells suspension of 10^6 cells ml^{-1}. Although the author reported a floc size reduction due to the beads addition, the effect of the physical (cells size and shape) and chemical (soluble content) algae characteristics on the strength and structure of the ballasted algae floc was not investigated. In addition, as the beads' presence allowed less turbulent flotation mechanisms (no saturated flow injection) compared to DAF, there is the potential to identify different optimal coagulation conditions that might generate additional advantages on top of the energy saving.

The present work investigates the performance of the BDAF technology applied to three different algae (*Scenedesmus obliquus*, *Chlorella vulgaris* and *Arthrospira maxima*)

compared to the conventional DAF. Optimal flocculation-flotation conditions were identified in terms of pH and coagulant dose depending on the specific cell morphology and AOM composition of each alga biomass. The impacts of microspheres inclusion into the algal biomass were assessed to compare floc characteristic between the two technologies. In addition, life cycle analysis (LCA) was applied to both DAF and BDAF harvesting option to investigate practical, economic and environmental benefits while moving from one system to the other.

2 Materials and Methods

Algal harvesting batch tests were performed at the stationary growth phase (maximum yield) where the cell morphology is homogeneous and the AOM has the greatest effect on the coagulation. First, the algae cultures were characterised for cell morphology and the AOM composition. Secondly, optimal coagulation conditions were identified in terms of pH, coagulant dose, residual cells, turbidity and zeta potential. Subsequently, the characteristics of the optimal algae floc were investigated for size, strength and fractal dimension.

2.1 Algal culture

The two green algae, *Scenedesmus obliquus* (276/42) and *Chlorella vulgaris* (211/BK), and the blue-green alga *Arthrospira maxima* (1475/9) commonly known as *Spirulina*, were obtained from the Culture Collection for Algae and Protozoa (CCAP) (Oban, UK). All algae were cultivated in glass tanks illuminated with two fluorescent light tubes, Sun-glo 20W and Arcadia 18W. *S. obliquus* and *C. vulgaris* were grown at 18ºC in Jaworski media (50 litres) under constant illumination and mixed using an aquarium pump. *A.maxima* was grown in Zarrouk media (25 litres) at 28 ºC and 16/8 hours light/dark cycle, with daily mixing by hand.

2.2 Algae suspension and AOM characterisation

Cell counting was performed manually using a light microscope with a haemocytometer or a Sedge-wick Rafter as appropriate. Algogenic organic matter (AOM) was characterised and extracted at the stationary growth phase after centrifugation and filtration (1µm) according to the methods described by Henderson *et al.* (2008a). Samples were characterised for protein content, carbohydrate content and dissolved organic carbon (DOC). Bovine serum albumin (BSA) and glucose were used for calibration of protein and carbohydrate content respectively and read at 750 nm (BSA) and 480 nm (glucose) absorbance using a Jenway 6505 UV/Vis spectrophotometer. A Shimadzu TOC-5000A (Malvern, UK) was used for DOC analysis. Charge density of the algal suspension was measured through zeta potential analysis (Malvern Zetasizer 2000HAS, Malvern, UK) by the addition of an increasing dose of PolyDADMAC (Sigma Chemicals, UK) with a defined charge density value equal to 6.2 meq g^{-1} (Sharp *et al*., 2006). Total suspended solids (TSS) were measured according to standard methods (APHA).

2.3 Harvesting performance

Jar test experiments were carried out using an EC Engineering DBT6 DAF jar tester (Alberta, CND). Separate experiments were carried out in duplicate at pH 5, 7 and 9, using aluminium sulphate ($Al_2(SO_4)_3$) as the coagulant. The DAF and BDAF tests were performed according to Henderson *et al.* (2008b) and Jarvis *et al.* (2009), respectively. Briefly, 1 litre of algal suspension was rapidly mixed for 2 to 3 minutes at 200 rpm, while varying coagulant doses were added and the pH was adjusted using a 0.1 M HCl (5 M in the case of *A. maxima*) and 0.1 M NaOH solution. Slow mixing (30 rpm) was then maintained for 15 minutes (flocculation period). Within the DAF system, air saturated deionised water buffered with 0.5 mM $NaHCO_3$ and 1.8 mM NaCl was supplied at 450 kPa and an equivalent recycle ratio of 10%. In the BDAF system, 300 mg l^{-1} of low-density glass beads (100 kg m^{-3}) obtained from

Trelleborg Emerson and Cuming Inc. (Mansfield, USA) were added to the system prior to coagulant addition. Algae flocs were then allowed to float for 10 minutes. Clarified samples were taken from the vessel base and characterised for residual cells, turbidity and zeta potential as previously described. Residual aluminium concentration was measured using a Perkin Elmer AAnalyst800 atomic absorption spectrometer (Waltham, USA).

2.4 Floc size and breakage

Jar testing of both systems was completed under verified optimum conditions of pH and coagulant dose. To create a growth and breakage floc profile, the algal particle size distribution was measured every minute using a Malvern Mastersizer2000 (Malvern, UK). A peristaltic pump was used to maintain a constant flow of 1.5 l h^{-1} from the jar, through the laser diffraction unit and back into the jar. The suspension was rapidly mixed (200 rpm) for 2 minutes while the coagulant dose and pH were adjusted. Flocculation conditions were then maintained at 30 rpm for 15 minutes. Subsequently, the mixing speed was adjusted to 30 rpm, 50 rpm, 75 rpm, 100 rpm, 150 rpm and 200 rpm, equivalent to mean velocity gradient (G) values of 7.4 s^{-1}, 15.9 s^{-1}, 29.3 s^{-1}, 45.2 s^{-1}, 82.9 s^{-1}, 128 s^{-1}, as determined using a conversion equation provided by the Mastersizer supplier, for an additional 15 minutes. Fractal dimension values (D_f) were obtained from a log - log plot of scattering intensity versus wave number considering the gradient of the straight line. Light energy intensity values were converted to raw scattering intensity using the software provided by the Mastersizer supplier.

2.5 Life cycle assessment

Life cycle assessment (LCA) was carried out for hypothetical full scale DAF and BDAF systems having a treatment capacity (Q) of 20000 m^3 d^{-1}, to compare the energy demand, carbon footprint and costs of the two systems. As the focus of this study is the comparison of

161 the two harvesting options (DAF and BDAF), the up- and downstream processes are excluded
162 from the analysis as they are assumed to be the same in both cases and therefore have no
163 effect on a comparative analysis. Calculations were performed for (1) operational carbon
164 emissions, based on the operational inputs (electricity, coagulant and glass beads) required to
165 harvest the algae biomasses, and (2) embodied carbon emissions, based on the two major
166 construction differences between the two systems: the saturator for DAF, and the
167 hydrocyclone for BDAF. Carbon emissions are calculated in terms of carbon dioxide
168 equivalent (CO_2e), a measure of the total global warming potential of greenhouse gases, using
169 standard carbon coefficient conversion factors (Table 1) and $kgCO_2e\ d^{-1}$ as the functional unit.
170 The cost assessment was completed using available data on average market prices and
171 information from personal communication with different suppliers.
172 The saturator design was assessed according to the guidelines and parameters reported by
173 Edzwald and Haarhoff (2012) for a volumetric air requirement equal to 7 ml l^{-1}: packed
174 saturator operating at 500 kPa (saturation gauge pressure), 55 l m^{-2} s^{-1} (mass hydraulic
175 loading), 9.95% recycle ratio (Q_r/Q), packing depth of 1400 mm and associated energy
176 consumption, out of any secondary losses, equal to 0.013 kWh m^{-3} of raw water flow (fresh
177 water). Equation 1 was used for the determination of the mass (M) of a cylindrical vessel with
178 hemispherical ends made of stainless steel A36

(1)

179 $$M = 2\pi r^2 (r + w) P \frac{\rho}{\delta} \quad (1)$$

180 where r is the saturator radius, w the packing depth, P the gauge pressure, ρ the steel density
181 (7800 kg m^{-3}) and δ the steel ultimate tensile strength (400Mpa). Christy®Pak polypropylene
182 pall rings (38 mm, 51 kg m^{-3}, 140 m^2 m^{-3}) were considered as packing material.

183 Conventional hydrocyclones operate at a pressure value between 50 and 300 kPa (Jun *et al.*,
184 2009) and have a total mass of stainless steel or cast iron, according to available commercial

information, between 8 and 45 kg for a design capacity between 10 and 25 $m^3 h^{-1}$. For the purpose of the LCA, a 150 kPa pressure drop (high efficient sand separator), 18 kg mass (stainless steel) and a treatment capacity equal to 0.02 Q, were assumed.

The energy demand for pumping water into both saturator and hydrocyclone units were estimated in terms of water-energy according to Equation 2

$$Pw = \frac{Q\ \rho\ g\ h}{\eta\ 3.60\ 10^6} \quad (2)$$

where Pw is the required daily power (kW), Q the water flow rate ($m^3 d^{-1}$), ρ the fluid density (1000 kg m^{-3}), g gravity (9.81 m s^{-2}), h the pressure drop (m head) and η the pump efficiency (70%).

The coagulant (aluminium sulphate, $Al_2(SO_4)_3$) dosage was calculated from the optimal doses determined in the present work. For the glass bead demand, assuming a treatment capacity of 850 $m^3 hr^{-1}$ and optimal bead concentration of 300 mg l^{-1}, 255 kg hr^{-1} of beads were required. However, when the system is in steady state 242 kg hr^{-1} of beads were recycled inside the system (95% bead recycling efficiency), with 13 kg hr^{-1} of new beads needed as 13 kg hr^{-1} (1.5 g m^{-3}) of beads remain in the harvested biomass.

3 Results and Discussion

3.1 Algal suspension characteristic

Key differences between the three algae were observed in terms of their surface area, AOM concentration and composition as well as charge density (Table 2). To illustrate, the surface area of *S. obliquus* was approximately double that of *C. vulgaris* at 49.5 and 28.3 μm^2 $cell^{-1}$, respectively. Compared to these two single cells algae, the filamentous *A. maxima* presented a significantly higher surface area with an average value close to 3720 μm^2 $cell^{-1}$. In terms of AOM, *S. obliquus* and *C. vulgaris* showed comparable DOC concentrations, while *A. maxima* reported higher values. For instance, the carbohydrate content of the two green algae ranged

between 4 and 5 mg l^{-1}, as glucose, while it was seven to ten times higher in *A. maxima* (38.18 ± 2.62 mg l^{-1} as glucose). In contrast, the proteins content was more consistent across the three algae, with *S. obliquus* at 6.31 ± 1.40 mg l^{-1}, *C. vulgaris* at 1.80 ± 0.09 mg l^{-1} and *A. maxima* at 5.24 ± 0.1 mg l^{-1} as BSA. At stationary growth phase the pH value of the algae suspensions was close to 7.5, 7.8 and 9.7 for *S. obliquus*, *C. vulgaris* and *A. maxima*, respectively. The related charge density measurement was equal to 1 ± 0.06, 4.6 ± 0.22 and 0.15 ± 0.02 peq μm^{-2} for the same algae with zeta potential values equal to or more negative than -30 mV. As the pH value was adjusted to the desire condition, the zeta potential, as well as the AOM concentration, reported little adjustments while clear pH-dependence was observed with charge density measurements. Growing in salt-free media, the charge density of green algae increased with the pH (Wang *et al.*, 2006), from 0.85 to 1.31 peq μm^{-2}, and from 2.76 to 5.52 peq μm^{-2}, at pH 5 and pH 9, for *S. obliquus* and *C. vulgaris*, respectively. In contrast, *A. maxima*, cultivated in a strong base solution, showed higher charge density values at lower pH (0.28 ± 0.02 peq μm^{-2} at pH and 70.31 ± 0.01 peq μm^{-2}at pH 5), congruent with polymeric hydrolysis reducing the charge of the functional groups (Kam and Gragory, 1999).

Overall, the three algae showed clear physical and chemical differences, which, according to previous investigations have the potential to impact on the specific harvesting performance (Zhang *et al.*, 2012; Henderson *et al.*, 2010). To compare, in terms of proteins:carbohydrates ratio, our results (Table 2) are in the same range as those reported by Henderson *et al.*, (2010) for equal or similar algae, like *Chlorella vulgaris* (0.4), *Microcystis aeruginosa* (0.6), *Asterionella formosa* (0.2) and *Melosira* sp. (0.2). As reported by the authors, between close algae strains, a higher proteins:carbohydrates ratio suggests a lower coagulant demand, having higher hydrophobicity and consequent lower charge density. Similarly, larger cells required higher coagulant doses as well as concentrated suspensions and growth media with a salinity concentration higher than 5 g l^{-1} (Knuckey *et al.*, 2006; Pieterse and Cloot, 1997). Hence,

from our analysis (Table 2), *A. maxima* is expected to require the highest coagulant dose compared to *S. obliquus* and *C. vulgaris*, having the largest surface area, high charge density and high salinity growth media. Between the two green algae, the higher proteins:carbohydrates ratio and the lower charge density of *S. obliquus*, suggest this alga will require less coagulant than *C. vulgaris*. However, the larger surface area and the higher proteins content might have a detrimental effect on the flocculation process (Henderson *et al.*, 2010) leaving *C. vulgaris* with the lowest coagulant demand.

3.2 Algal removal and coagulant demand

High algal cell recovery (≥99%) was achieved using both harvesting systems. However, significant differences for optimal coagulant dose and zeta potential were observed in relation to the algal strain and the pH value used (Figure 2). To illustrate, within the DAF system (Figure 2 – left column), *S. obliquus* showed complete removal at increasing coagulant demand for pH 5, pH 7 and pH 9 at zeta potential values lower than 15mV, 8mV and -10mV, respectively. Similarly, *C. vulgaris* coagulant demand increased with the pH, but in all experiments optimal removal occurred at neutral or negative zeta potential values. Despite the same range of zeta potential observed with the green algae, *A. maxima* showed different behaviour. In DAF conditions, algae separation predominately accrued by sedimentation instead of a flotation mechanism evidenced through visual observation of the flocs being too heavy to be lifted by the air bubbles injected at the tests air to solids ratio used. Hence, after an initial flotation they started to settle, suggesting DAF to be inappropriate for high density flocs (Jarvis *et al.*, 2009). At the highest pH condition, the zeta potential value slightly changed with increasing coagulant doses, remaining close to the initial value of -38 mV which is congruent with dissociation models for coagulants demonstrating that aluminium is in its

precipitated hydroxide form at pH 9. At pH 7, complete clarification was obtained at -15mV, while at pH 5 the optimal zeta potential value was close to 0 mV.

Separation trials performed under a BDAF set up achieved the same cell recovery observed within the DAF experiment but at lower coagulant doses (Figure 2 – right column). For instance, coagulant reductions of 40 %, 14 % and 22 % where observed in the case of *S. obliquus* when operated at pH 5, 7 and 9 respectively. In contrast, no significant saving was observed with *C. vulgaris* at pH 5, while 45 % and 75 % reduction was obtained at pH 7 and pH 9, respectively. *A. maxima* showed removal efficiency below 80 % only at pH 9. At pH 7 and pH 5, complete removal was obtained at zeta potential values close to -32 mV and -26 mV, respectively. Coagulant savings reached 95 % at pH 5, while remaining between 25 % and 30 % for the other two conditions.

Overall, DAF was effective only on *S.obliquus* and *C. vulgaris* separation, while BDAF enables an efficient flotation for both green algae and the filamentous cyanobacteria. Both systems reported poor separation (<80 %) at low coagulant doses (< optimal dose), however, with ballasting agents the low efficiency was more due to uncompleted algae-beads floc formation rather than floc breakage as observed during DAF separation consistent with the lower levels of energy dissipation encountered in BDAF (Jarvis *et al.*, 2011). In all experimental conditions, optimum cell recovery occurred at pH 5 and the coagulant demand increased with the pH in all algae suspensions. As organic particles, the optimal coagulation condition of microalgae requires a low pH level (~pH 5-6) where charge neutralisation mechanisms are dominant (Stumm and Morgan, 1962). Similar behaviour was reported in the work of Henderson *et al.* (2010) where harvesting *C. vulgaris* at pH 7 required four times more coagulant than at pH 5. In agreement with previous work, conventional flotation achieved complete algal separation as the zeta potential approached neutral or positive values (Henderson *et al.* 2008b); however, in the ballasted flotation experiments, the same removal

284 occurred at more negative zeta potential values as a consequence of the reduced coagulant
285 dosage.
286 Aluminium sulphate was an effective coagulant and residual aluminium concentration in all
287 clarified samples was always equal to or less than 1 mg l^{-1}. In terms of optimal coagulant
288 demand, the experimental results confirmed initial considerations (§ 3.1) based on cell
289 characteristics and AOM composition and showing values within the range of similar
290 freshwater microalgae (Henderson *et al.*, 2010; Molina Grima *et al.*, 2003; Edzwald, 1993). *A.*
291 *maxima* required the highest amount of coagulant (≥ 60 mg Al l^{-1}, at pH 5, DAF), followed by
292 *S. obliquus* (25 mg Al l^{-1}, at pH 5, DAF) and *C. vulgaris* (2 mg Al l^{-1}, at pH 5, DAF). Between
293 the two green algae, the larger surface area and the higher proteins contents responsible for
294 protein complexation with aluminium, justify the higher coagulant dosage observed in *S.*
295 *obliquus* compared to *C. vulgaris* despite the lower charge density (Henderson *et al.*, 2010).
296 According to our observations, the BDAF has the potential to generate a more concentrated
297 final algae paste than DAF. After conventional flotation of *S. obliquus* the solid content of the
298 concentrated biomass was between 1 and 2% in term of TSS (biomass concentrated in the top
299 10 ml of the 1l jar) which is within expected values (Rawat *et al.*, 2013). For the same final
300 volume, the TSS percentage obtained using BDAF was close to 5% due to the presence of the
301 glass beads. Assuming an efficient post flotation beads separation by using a hydrocyclone
302 with 20% (vol.) underflow (Jianghua *et al.*, 2009), the estimated final TSS content would
303 range from 5 to 10%.
304
305 *3.3 Floc growth and strength profiles*
306 Floc comparison was made based on equivalent media volumetric diameter (d_{50}). Comparing
307 the steady state floc size achieved during chemical (pre DAF) and ballasted flocculation, *S.*
308 *obliquus* did not show significant differences as the d_{50} remained close to 130.3 ± 11.2 µm. In

309 contrast, *C. vulgaris* reported floc size reduction, from 223.6 ± 14.5 µm to 113.8 ± 13.2 µm,
310 while *A. maxima* floc size grew from 103.3 ± 16.5 µm to 146.3 ± 14.6 µm. Floc size reduction
311 due to the addition of microspheres was first reported by Jarvis *et al.* (2009), who linked this
312 to a consequent reduction of the floc strength compared to conventional aggregates. However,
313 the peculiarity of *A. maxima* (filamentous algae) suggests that the physical property of the cell
314 has a key role in the algae-bead floc formation/structure, as observed in conventional algal
315 aggregation (Pieterse and Cloot, 1997). Despite the flocculation condition investigated, *S.*
316 *obliquus* and *C. vulgaris* achieved steady state floc size after 9 to 12 minutes, while *A.*
317 *maxima* required less than 4 minutes (Annex A). Accordingly, the *C. vulgaris* floc growth rate
318 ranged between 10 µm min^{-1} and 60 µm min^{-1} during the first 5 minutes and between 1 µm
319 min^{-1} and 10 µm min^{-1} afterwards until steady state was reached. No flocculation time-lag was
320 observed in any of the experiments, suggesting that an optimal coagulant dose was provided
321 (Clasen *et al*., 2000). During the first 2 minutes at a high shear rate (while coagulant was
322 added and the pH level adjusted), an instant floc formation was observed for *S. obliquus* and
323 *A. maxima*. Subsequently, the d_{50} value gradually decreased to a steady state floc size.
324 Using the steady state floc size as an indication of the floc strength (Jarvis *et al*., 2005), *C.*
325 *vulgaris* formed the strongest floc, followed by *S. obliquus* and *A. maxima* in the DAF
326 system. Conversely, in the ballasted system, the sequence was reversed with the strongest floc
327 associated to *A. maxima*, followed by *S. obliquus* and *C. vulgaris.* Extending the analysis to
328 the flocs behaviours when exposed to an increasing shear rate (Figure 3), the chemically
329 induced floc of the two green algae showed a clear resistance of up to 16 G (50 rpm). As the
330 shear rate increased, the degradation rates increased. The same correlation was observed using
331 microspheres, but no floc breakage resistance was detected at low shear rates confirming a
332 more fragile floc.

A more detailed analysis of the floc strength between the two systems was possible comparing the floc strength coefficient (log C) and the floc strength constant (κ), as well as the floc response to increased shear rate exposure. The floc strength coefficient and constant were extrapolated from Figure 3 as described by Jarvis *et al.* (2005). The first, represented by the y-axis intercept, gives an indication of the floc strength. The second, the gradient of the slope, reveals information on floc breakage mechanisms: floc fragmentation for κ values close to 0.5 and floc erosion for values between 1 and 2 (Li *et al.*, 2006). Compared to the conventional flotation system, the addition of glass beads did not change the strength coefficient of *S. obliquus* (Table 3). However, it generated an 18% reduction with *C. vulgaris* and 3% improvement with *A. maxima*. This confirmed previous observations based on steady state floc size, as the beads addition affects the most *C. vulgaris*' floc strength and reinforced *A. maxima*. The calculated floc strength's constant values indicated fragmentation as the main floc breakage mechanism in both systems, which is consistent with other observations on similar freshwater algae (Table 3). Furthermore, exposed to an increase shear rate, the d_{50} showed clear reduction from values higher than 100µm to lower sizes as a result of floc fragmentation (Figure 4). However, as observed with similar algae (Henderson *et al.*, 2006), the two green algae showed some evidence of an erosion mechanism after 15 minutes of exposure to an increased shear rate, with a small increment in the volume of particle sizes between 4 and 6 µm (Figure 4 A and C). Furthermore, at ballasted conditions, *C. vulgaris* reported a small increment of large particle sizes (450-650 µm) suggesting floc re-structuring during the breakage (Figure 4 D). This reinforced the possibility that high post-separation beads recovery can be achieved as the algae-beads floc break, enabling beads recycling and algae concentrations at the same time. Efficient bead separation was observed at bench scale at a high shear rate (200 rpm) for all three algae tested. However, the ratio between clearly separated and algae-linked beads was not determined.

A microscopic analysis of the algae flocs confirmed that beads interact differently with unicellular and filamentous algae (Figure 5). In the first case, the algae cells were distributed around the bead's surface (Figures 5, A2 and B2) creating a compact structure (Jarvis *et al.*, 2009). In contrast, filamentous algae tend to create a more structured agglomeration where microspheres are in a pivoted position (Figure 5, C2). These observations are confirmed by fractal dimension (D_f) analysis (Figure 6). When moving from the DAF to BDAF systems, the D_f increases from 2.18 ± 0.05 to 2.25 ± 0.03 and from 2.43 ± 0.02 to 2.55 ± 0.04 for *S. obliquus* and *C. vulgaris*, respectively, suggesting a similar compact structure. In contrast D_f decreased from 2.45 ± 0.08 to 2.25 ± 0.04 in the case of *A. maxima* endorsing the change in structure (from a compact aggregation to a more open one). Exposed to increasing shear rate, *S. obliquus* showed D_f reduction to 2 ± 0.01 and 2.04 ± 0.04 with and without beads, respectively, from 100 rpm and afterwards (Figure 6). Similarly, the fractal dimension of *A. maxima* decreased with the shear rate. However, resistance to shear rate of or less than 100 rpm was observed only without the presence of beads. In contrast, despite the flocculation condition provided, *C. vulgaris* D_f increased with the shear rate. Visual observations of samples exposed to a high shear rate (200 rpm for 15 minutes) showed an algal re-suspension associated with the presence of a clear glass bead layer on the surface. This supports the algae-bead floc breakage and suggests that the re-structuring mechanism observed within *C. vulgaris* might affect only the algae cells as microspheres float on the surface allowing successful beads recovery.

3.4 Life cycle assessment

The results from the LCA show that, compared to the traditional DAF technology, the adoption of BDAF allows up to 33 %, 58 % and 44 % carbon emission saving for *S. obliquus*, *C. vulgaris* and *A. maxima*, respectively (Table 4). Most of the carbon savings come from the

lower coagulant demand associated with the system as the coagulant dosage was always the main contributing factor to operational carbon emissions (Figure 7). In terms of embodied carbon, the BDAF technology allows a saving close to 300 kg CO_2e, corresponding to a 40% reduction compared to the DAF system. The contributions of the saturator and the hydrocyclone to the total embodied carbon were nearly equal. However, significant differences were observed between the embodied carbon of the two associated pumps. As the hydrocyclone works at lower pressure and treats 5 times less effluent than the saturator, the BDAF unit required a smaller pump which generated a 66 % CO_2e reduction; however, this saving was partially outweighed by the glass beads addition with more than 200 kg of CO_2e (50 % of the total BDAF embodied carbon).

From the economical perspective, the high price of glass beads (70-80 £ kg^{-1}) limited the cost reduction. For instance, on a 10 year bases, the conventional life time of a pump (Skongaard and Nielsen, 2004), *S. obliquus* and *A. maxima* reported economic benefits equal to 1.2 and 18.4 million £, while *C. vulgaris* was more economically harvested using the DAF unit, because of the lower coagulant demand required compared to the other algae. Overall, compared the conventional DAF system, the BDAF technology was found to be more sustainable in terms of carbon footprint and to offer significant economic savings depending on the algae biomass used and the price of the flouting ballasting agent.

4 Conclusions

Ballasted Dissolved Air Flotation (BDAF) was demonstrated to be a more feasible and sustainable microalgae harvesting option compared to the conventional flotation technology. The adoption of floating microspheres as ballasting agents (1) allowed significant coagulant saving, (2) showed a more reliable technology benefitting from a reduced level of energy dissipation within the flotation chamber, and (3) lowered the overall carbon emissions and (4)

the process costs. The comparison between the conventional and the ballasted floc structure and strength revealed that the algae-beads aggregation was more affected by the cell's morphology than the AOM. Single cell algae formed compact and strong algae-bead flocs, while filamentous species resulted in a more expanded and inferior structure. However, the AOM composition was confirmed to be a key parameter for the determination of optimal flocculation conditions, as it affected the coagulant demand in both DAF and BDAF technologies. Further research focused on the microspheres recovery process is required to optimise hydrocyclone configuration in order to guarantee beads recovery and energy/costs savings.

Acknowledgments

The authors would like to thank the EU Framework 7 project Advanced Technologies for Water Resources and Management (ATWARM - Marie Curie Initial Training Network, No. 238273) as well as the Engineering and Physical Sciences Research Council (EPSRC), Anglian Water, Severn Trent Water and Scottish Water for their financial and intellectual support, and Northern Ireland Water where part of the carbon research was carried out.

References

Christenson, L., Sims, R., 2011. Production and harvesting of microalgae for wastewater treatment, biofuels, and bioproducts. Biotechnol. Adv. 29 (6), 686-702.

Clasen, J., Mischke, U., Drikas, M., Chow, C., 2000. An improved method for detecting electrophoretic mobility of algae during the destabilisation process of flocculation: flocculant demand of different species and the impact of DOC. Journal of Water Supply: Research and Technology - AQUA 49 (2), 89-101.

Desjardins, C., Koudjonou, B., Desjardinis, R., 2002. Laboratory study of ballasted flocculation. Water Res. 36 (3), 744-754.

433 Edzwald, J.K., 1993. Algae, bubbles, coagulants, and dissolved air flotation. Water Sci. and
434 Technol.27 (10), 67-81.
435 Edzwald, J.K., Haarhoff, J., 2012. Air saturation. In: Dissolved Air Flotation For Water
436 Clarification, pp. 3.1-3.36. J. Am. Water Works Assoc.
437 Granados, M.R., Acien, F.G., Gomez, C., Fernandez-Sevilla, J.M., Molina Grima, E., 2012.
438 Evaluation of flocculants for the recovery of freshwater microalgae. Bioresourc.
439 Technol. 118, 102-110.
440 Henderson, R. K., Baker, A., Parsons, S. A., Jefferson, B., 2008a. Characterisation of
441 algogenic organic matter extracted from cyanobacteria, green algae and diatoms. Water
442 Res. 42 (13), 3435-3445.
443 Henderson, R. K., Parsons, S. A., Jefferson, B., 2008b. Successful removal of algae through
444 the control of zeta potential. Separ. Sci. Technol. 43 (7), 1653-1666.
445 Henderson, R., Parsons, S. A., Jefferson, B., 2010. The impact of differing cell and algogenic
446 organic matter (AOM) characteristics on the coagulation and flotation of algae. Water
447 Res. 44 (12), 3617–3624.
448 Henderson, R., Sharp, E., Jarvis, P, Parsons, S. A., Jefferson, B., 2006. Identifying the linkage
449 between particle characteristics and understanding coagulation performance. Water Sci.
450 Technol.: Water Supply 6 (1), 31-38.
451 Jarvis, P., Buckingham, P., Holden, B., Jefferson, B., 2009. Low energy ballasted flotation.
452 Water Res. 43 (14), 3427-3434.
453 Jarvis, P., Jefferson, B., Gregory, J., Parsons, S. A., 2005. A review of floc strength and
454 breakage. Water Res. 35 (14), 3121-3137.
455 Jarvis, P., Martin, J., Winspear, T. and Jefferson, B., 2011. Ballasted flotation with glass
456 microspheres for removal of natural organic matter. Separ. Sci. Technol. 46 (16), 2489-
457 2495.

458 Jianghua, Y., Qitao, Y., Kim, Y., 2009. Performance analysis of a hydrodynamic separator for
459 treating particulate pollutants in highway rainfall runoff. Environ. Eng. Res. 14 (4), 262-
460 269.
461 Jun, H., Lian-suo, A., Zhi-quan, W., 2009. Study on application and operation optimization of
462 hydrocyclone for solid-liquid separation in power plant. Proceeding of the World
463 Congress on Engineering and Computer Science (WCECS) San Francisco, USA, 1.
464 Kam, S., Gregory, J., 1999. Charge determination of synthetic cationic polyelectrolytes by
465 colloid titration. Colloids and Surf.159 (1), 165-179.
466 Knuckey, R. M., Brown, M. R., Robert, R., Frampton, D. M. F., 2006. Production of
467 microalgal concentrates by flocculation and their assessment as aquaculture feeds.
468 Aquacult. Eng.35 (3), 300-313.
469 Lee, D. H., 2011. Algal biodiesel economy and competition among bio-fuels.
470 Bioresourc.Technol.102 (1), 43-49.
471 Li, T., Zhu, Z., Wang, D., Yao, C., Tang, H., 2006. Characterization of floc size, strength and
472 structure under various coagulation mechanisms. Powder Technol. 168 (2), 104-110.
473 Li, L., Gao, N., Deng, Y., Yao, J., Zhang, K., 2012. Characterization of intracellular and
474 extracellular algae organic matters (AOM) of Microcystic aeruginosa and formation of
475 AOM-associated disinfection byproducts and odor and taste compounds. Water Res.46
476 (4), 1233-1240.
477 Molina Grima, E., Berlarbi, E. H., Acién Fernández, F. G., Robles Medina, A., Chisti, Y.,
478 2003. Recovery of microalgae biomass and metabolites: process options and economics.
479 Biotechnol. Adv. 20 (7-8), 491-515.
480 Pieterse, A. J., Cloot, A., 1997. Algal cells and coagulation, flocculation and sedimentation
481 processes. Water Sci. and Technol. 36 (4), 111-118.

Pivokonsky, M., Kloucek, O., Pivokonska. L., 2006. Evaluation of the production, composition and aluminium and iron complexation of algogenic organic matter. Water Res. 40 (2), 3045-3052.

Rawat, I., Kumar, R.R., Mutanda, T., Bux, F., 2013. Biodiesel from microalgae: a critical evaluation from laboratory to large scale production. Appl. Energy 103, 444-467.

Sharp, E.L., Jarvis, P., Parsons, S.A., Jefferson, B., 2006. Impact of fractional character on the coagulation of NOM. Colloids Surface A. 286 (1-3), 104–111.

Stumm, W., Morgan, J. J., 1962. Chemical aspects of coagulation. J. Amer. Water Works Assoc. 54 (8), 971-994. Wang, Y., Hubbe, M.A., Sezaki, T., Wang, X., Rojas, O. J., Argyropoulos, D. S., 2006. The role of polyampholyte charge density on its interactions with cellulose, Nordic Pulp and Paper Research Journal 21 (5), 158-165.

Zhang, X, Amendola, P., Hewson, J. C., Sommerfeld, M. and Hu, Q., 2012. Influence of growth phase on harvesting of Chlorella zofingienis by dissolved air flotation, Bioresourc. Technol. 116, 477-484.

DEFRA and DECC, 2013. Greenhouse gas conversion factor repository. Department for Environment, Food and Rural Affairs and Department of Energy and Climate Change. http://www.ukconversionfactorscarbonsmart.co.uk/ (accessed 17 June 2013).

Hammond, G., Jones, C., 2011. Inventory of carbon and energy, version 2.0. Sustainable Energy Research Team (SERT), University of Bath. http://www.bath.ac.uk/mech-eng/sert/embodied/ (accessed 25 July 2011).

OFWAT, 2010. Playing our part: how can we cut greenhouse gas emissions in the water and sewerage sectors? The Water Services Regulation Authority. http://www.ofwat.gov.uk/sustainability/climatechange/prs_web_1007emissions (accessed 19 July 2012).

Skongaard, A., Nielsen, C.B., 2004. Pump handbook. Grundfos Managmnent http://net.grundfos.com/doc/webnet/mining/_downloads/pump-handbook.pdf (accessed 30 September 2013).

UM, 2011. CCaLC© manual, version 2.0, carbon calculations over the life cycle of industrial activities. The University of Manchester. http://www.ccalc.org.uk/ (accessed 17 August 2011).

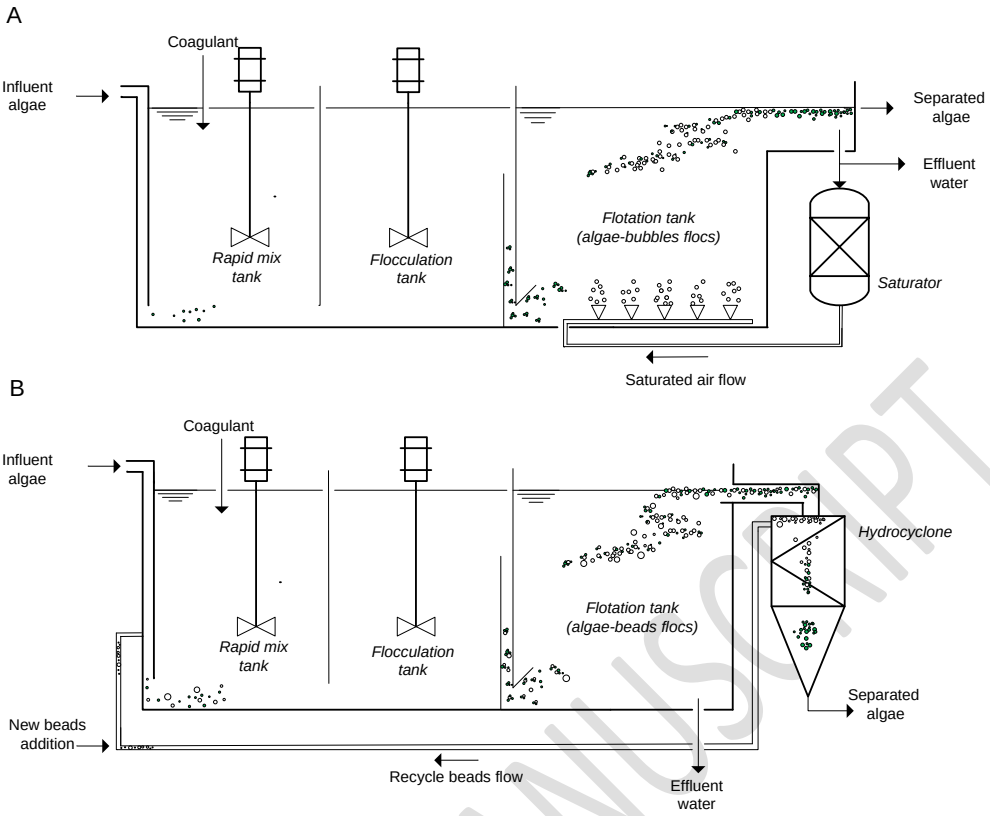

517

518 Figure 1 Schematic representation of Dissolved Air Flotation (A) and Ballasted Dissolved Air
519 Flotation (B) systems.
520

521

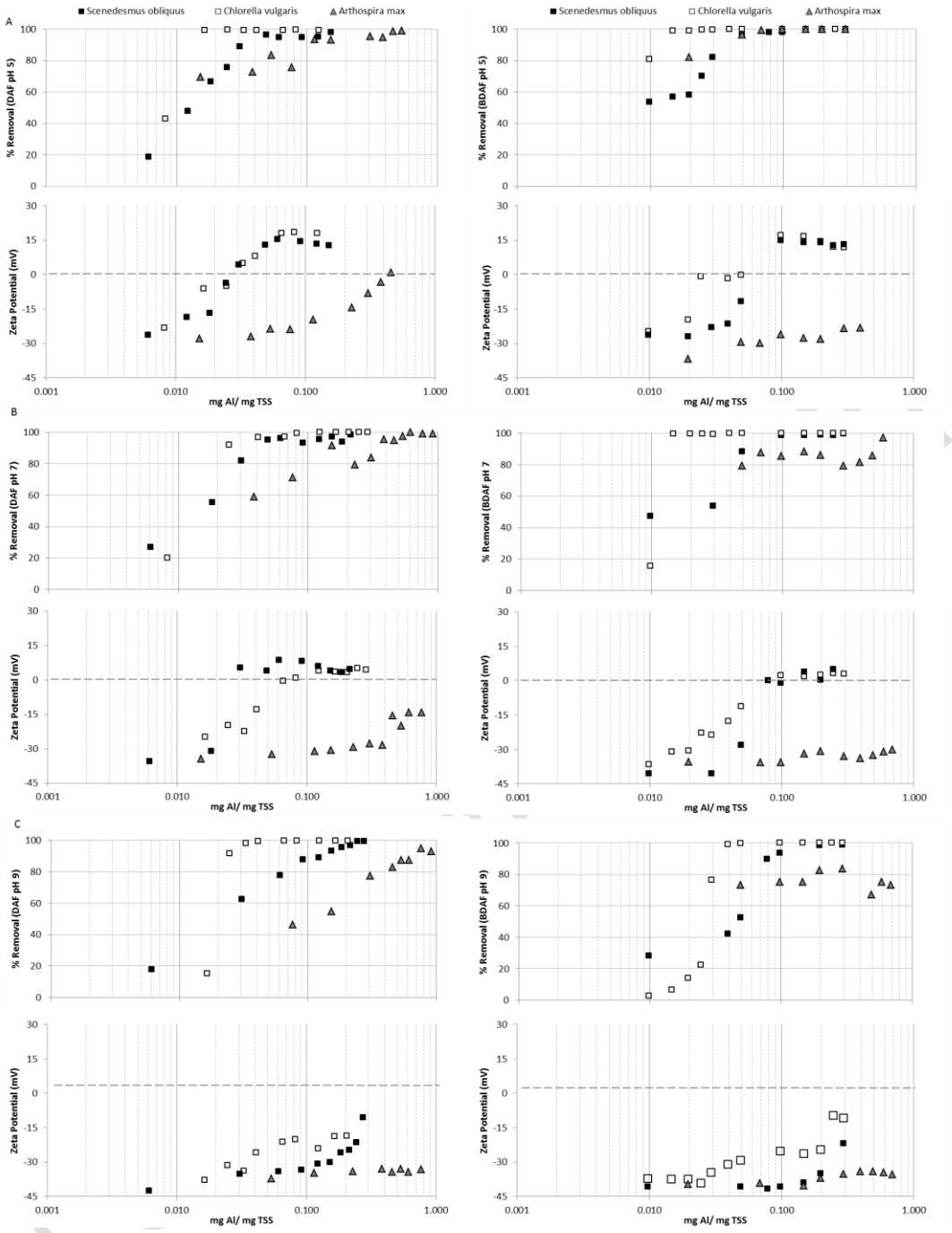

522

523 Figure 2 Dose response curve and corresponding zeta potential values for *S. obliquus*, *C.*
524 *vulgaris* and *A. maxima*, for DAF (right column) and BDAF (left column) system at pH 5 (A),
525 pH 7 (B) and pH 9 (C).

526

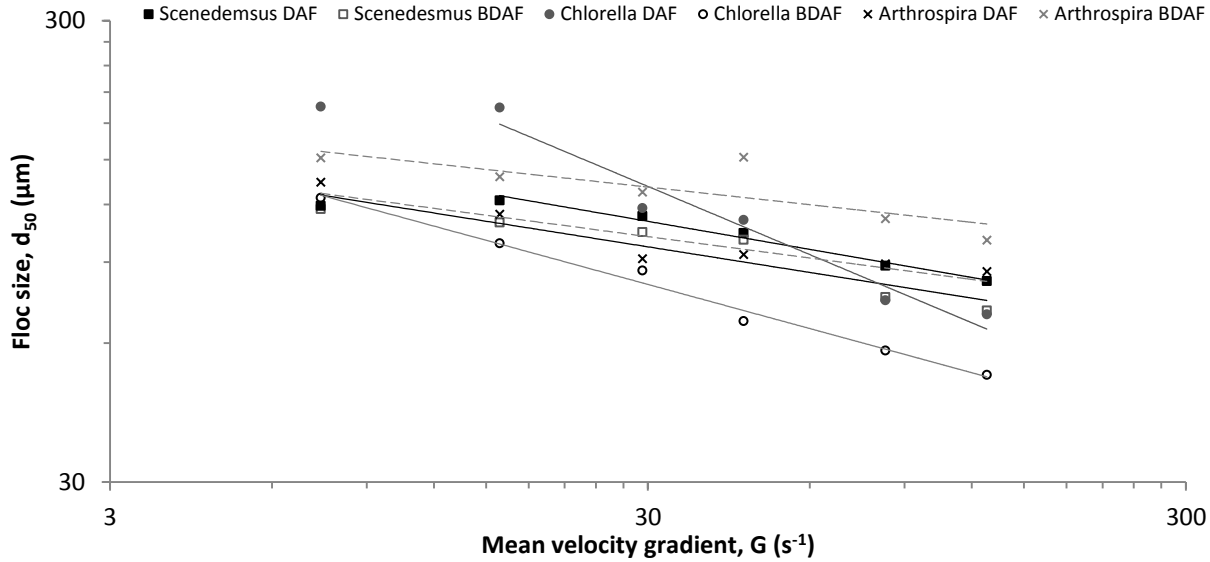

527

528 Figure 3 Log log plot of steady state floc size vs increasing shear rate plotted as G, with and
529 without microspheres addition.

530

531

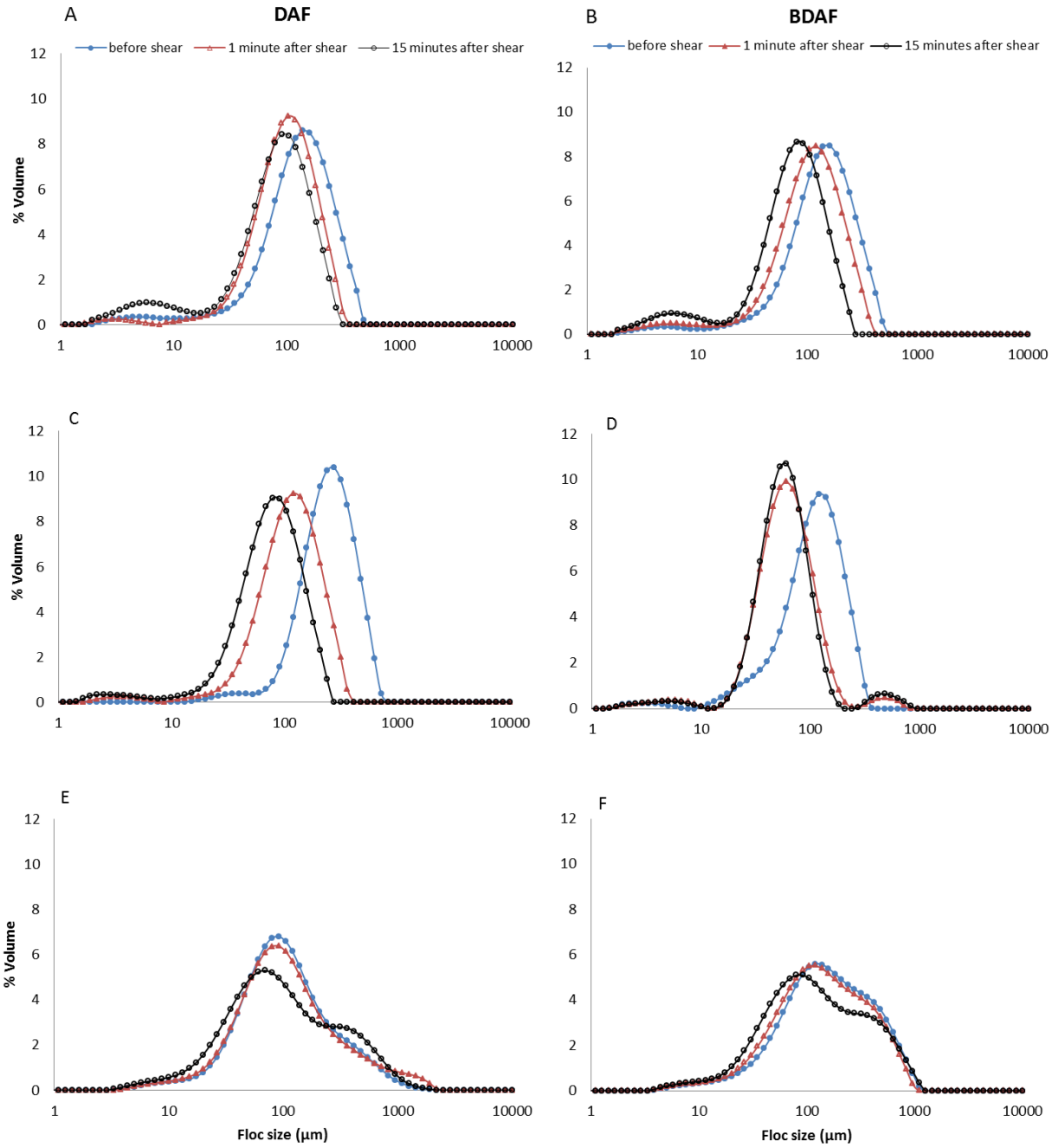

532

533 Figure 4 Floc breakage profile for DAF (left column) and BDAF (right column) system, of *S.*
534 *obliquus* (A and B), *C. vulgaris* (C and D) and *A. maxima* (E and F), before and after
535 exposure to a shear rate of 200 rpm.

536

537

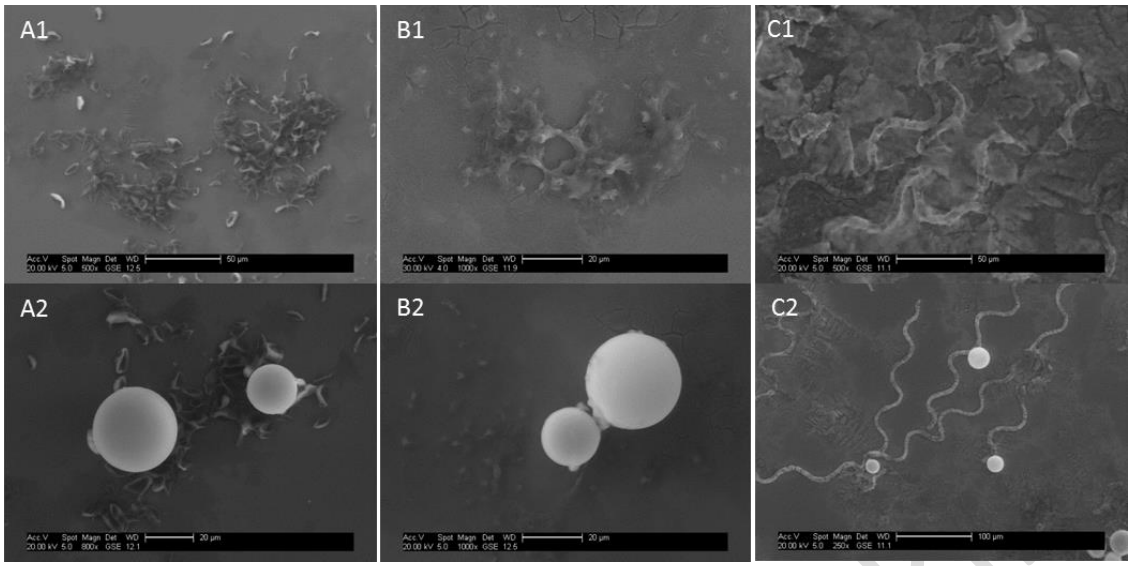

Figure 5 Algae floc images ESEM Fei XL30 for *S. obliquus* (A), *C. vulgaris* (B) and *A. maxima* (C) in conventional flocculation condition (1) and in ballasted condition (2).

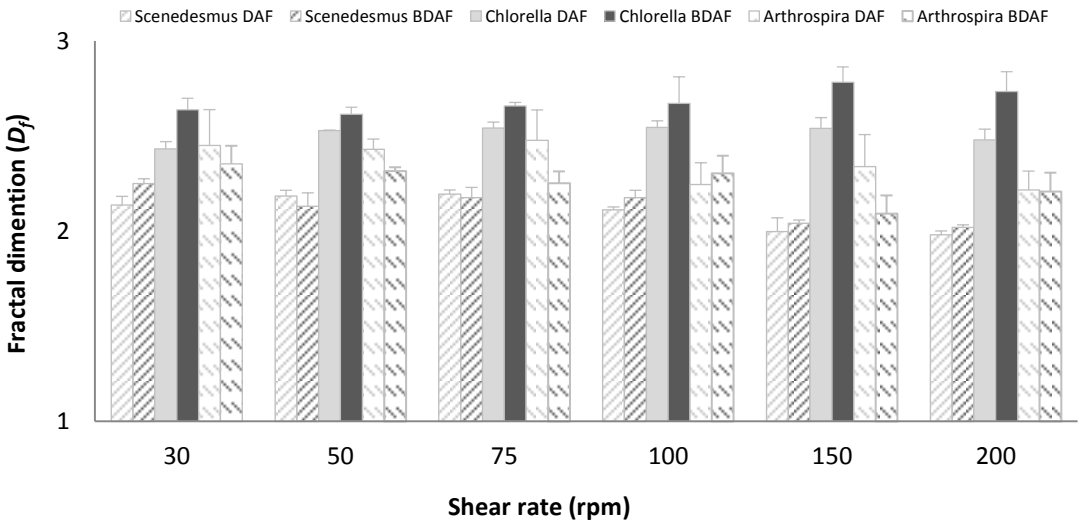

544

545 Figure 6 Fractal breakage profile for DAF (light grey) and BDAF (dark grey) system, of *S.*
546 *obliquus*, *C. vulgaris* and *A. maxima* exposed for 15 minutes at increasing shear rates.

547

548

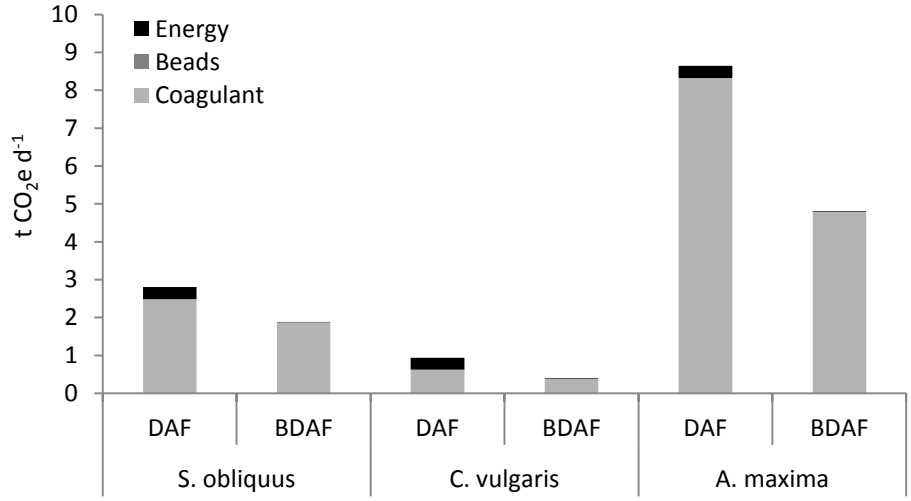

549

550 Figure 7 Operational carbon footprint comparisons between DAF and BDAF for the three
551 algae *S. obliquus*, *C. vulgaris* and *A. maxima.*

552

553

554 Table 1 Carbon factors

Carbon factors	Units	Value	*References*
Stainless steel	$kgCO_2e\ kg^{-1}$	3.23	*UM, 2011*
Cast iron[a]	$kgCO_2e\ kg^{-1}$	1.520[a]	
Polypropylene[b]	$kgCO_2e\ kg^{-1}$	2.334[b]	
Aluminium sulphate[c]	$kgCO_2e\ kg^{-1}$	0.493[c]	
Glass beads[d]	$kgCO_2e\ kg^{-1}$	0.900[d]	*Hammond and Jones, 2011*
Electricity[e]	$kgCO_2e\ kWh^{-1}$	0.484[e]	*DEFRA/DECC, 2013*

555 *[a]The emission factor for cast iron is for the product at the factory gate; [b]The emission factor is for polypropylene*
556 *fibres; [c]The emission factor for aluminium sulphate is for the product in powder form at the factory gate; [d]The*
557 *emissions factor is for UK primary glass (cradle-to-gate). Emissions from beads loss were excluded from the*
558 *analysis as they had no significant impact on the overall balance; [e]The emissions factor is for UK electricity and*
559 *accounts for emissions from generation as well as for losses in transmission and distribution.*
560

561

562 Table 2 Characterisation of microlgal suspention used in jar tests. Algae samples were taken
563 at the stationary growth phase and diluted with deionised water, buffered with 0.5 mM
564 $NaHCO_3$ and 1.8 mM NaCl, to reach the reported concentration.

	Parameter	*S. obliquus*	*C. vulgaris*	*A. maxima*
Algae suspension	Concentration (cells ml^{-1})	$2x10^6 \pm 1x10^5$	$2x10^6 \pm 1x10^5$	$2x10^4 \pm 1x10^3$
	Particle shape	spindle	spherical	filament
	Particle size[a] (µm)	6 w; 10.5 l	4.5 Ø	4.5 Ø; 300 l
	Surface area[a] (μm^2 $cell^{-1}$)	49.5	28.3	3719.9
	Solids (mg TSS l^{-1})	174 ± 14	112 ± 14	117 ± 19
	Turbidity (NTU[b])	124 ± 5	40 ± 8	105 ± 10
	pH	7.5 ± 0.2	7.8 ± 0.1	9.7 ± 0.2
	Zeta Potential (mV)	-34.6 ± 6.0	-30.5 ± 1.2	-44.2 ± 7.8
	Charge density (peq $cell^{-1}$)	0.050 ± 0.003	0.130 ± 0.006	0.564 ± 0.061
AOM	DOC (mg l^{-1})	3.81 ± 1.81	4.77 ± 0.59	100.5 ± 0.70
	Proteins:DOC ratio	1.91 ± 0.76	0.40 ± 0.33	0.39 ± 0.04
	Carbohydrates:DOC ratio	1.69 ± 0.77	0.92 ± 0.25	0.05 ± 0.01
	Poteins:Carbohydrates ratio	1.24 ± 0.06	0.43 ± 0.16	0.13 ± 0.01

565 [a]average value; [b]Nephelometric Turbidity Unit.

566

567

Table 3 Comparison between floc strength constants, floc strength coefficients and floc size reduction of different microalgae under different flocculation conditions.

Particles	Experiment condition			Floc strength			References
	Coagulant	Dose (mg l^{-1})	pH	log G	ɤ	%[a]	
Unballasted							
Scenedesmus obliquus	Al	40	5	2.34	0.20	38	*Current work*[b]
Chlorella vulgaris	Al	10	5	2.84	0.49	72	
Arthrospira maxima	Al	134	5	2.23	0.15	8	
Chlorella vulgaris	Al	-	5	3.82	0.89	89	*Henderson et al., 2006*
Microcystis aeruginosa	Al	0.7	6	2.95	0.26	70	*Gonzalez Torres and Henderson, 2013*[c]
	Al	1	7	3.09	0.39	78	
	Fe	3	6	3.39	0.39	73	
	Fe	3	7	3.42	0.39	63	
	Al	5	6	3.12	0.33	55	
	Al	4	7	2.95	0.21	52	
	Fe	20	6	2.98	0.02	9	
	Fe	50	7	3.10	0.13	32	
NOM	Al	-	5.5	2.81	0.21	50	*Henderson et al., 2006*
NOM	Fe	8	4.5	-	-	66	*Jarvis et al., 2009*
Ballasted							
Scenedesmus obliquus	Al	30	5	2.34	0.23	44	*Current work*[b]
Chlorella vulgaris	Al	6	5	2.37	0.33	51	
Arthrospira maxima	Al	77	5	2.30	0.13	22	
NOM	Fe	8	4.5	-	-	75	*Jarvis et al., 2009*

[a]Floc size reduction compared to original size (steady state) after 15 minutes at shear rate of 200 rpm; [b]Differences with previously reported optimal coagulant doses are related to differences in the AOM composition of batches of algae used in the two experiments at different times; [c]Gonzalez Torres, A., Henderson, R.K., (2013). Personal communication, University of New South Wales, Australia.

576 Table 4 Carbon footprint and cost analysis of the DAF and BDAF systems.

Inputs	Materials	Carbon emissions[a]		Costs	
		DAF	BDAF	DAF	BDAF
Embodied		*kg CO_2 e*		*£$_{capital\ costs}$*	
Saturator	Stainless steel[b]	48	-	15000[c]	-
Packing material	Polypropylene[d]	119	-	800[e]	
Hydrocyclone	Stainless steel[f]	-	58	-	3000[c]
Beads	Glass[g]	-	230	-	15300[h]
Pump[i]	Cast iron	623	208	7500	1500
Subtotal		***790***	***496***	***23300***	***19800***
Saving			***295***		***3500***
Operational		*kg CO_2e d^{-1}*		*£ d^{-1}*	
Energy[j]	Electricity	317	12	92	3
Coagulant *(S. obliquus)*	Aluminium sulphate[k]	2485	1864	4032	3024
Coagulant *(C. vulgaris)*		621	373	1008	605
Coagulant *(A. maxima)*		8324	4783	13507	7762
Beads	Glass[g]	-	12	-	780[h]
Saving (10 year life time)		*t CO_2e*		*millions £*	
S. obliquus			3340		1.2
C. vulgaris			1979		-1.1
A. maxima			13996		18.4

577 *[a]calculated applying the carbon factors reported in table 1; [b]15 kg of stainless steel calculated from*
578 *equation 1; [c]average market price for full operating unit (online search); [d]51 kg polypropylene*
579 *according to the information provided by Christy®Catalytics for Christy Pak 1 Polypropylene Pall*
580 *Rings; [e]personal communication from supplier Christy®Catalytics; [f]18 kg as reported in the material*
581 *and methods (§ 2.5); [g]calculations based on the information reported in the material and method (§*
582 *2.5); [h]personal communication from supplier Trelleborg Offshore, Boston; [i]carbon emissions based on*
583 *410 kg and 137 kg of cast iron DAF and BDAF respectively according to commercial information*
584 *provided by Grundfos CAPS (costs were also provided); [j]electricity costs of 0.14 £ kWh^{-1} (average UK*
585 *value); [k]carbon emissions based on data reported in table 3, while costs are based on average market*
586 *prices (Granados et al., 2012).*
587

588

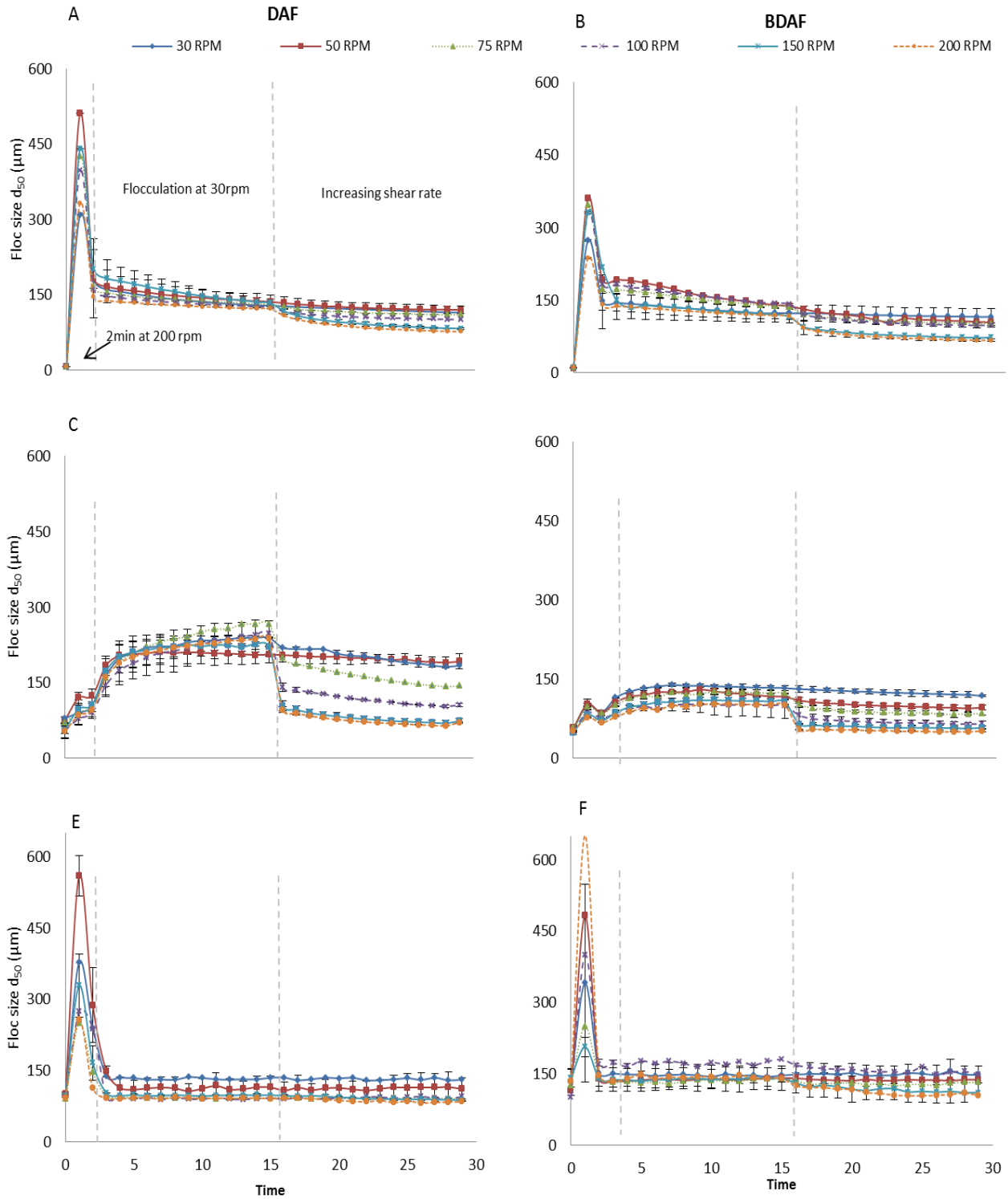

589

590 Figure A.1 Floc growth and breakage profile for DAF (left column) and BDAF (right column)
591 system, of *S. obliquus* (A and B), *C. vulgaris* (C and D) and *A. maxima* (E and F) at
592 increasing shear rate (on support of paragrph 3.1)

593

594